

1 ***Supporting Information***

2 **Fe(III)-complex mediated bacterial cell surface immobilization of**  
3 **eGFP and enzymes**

4 Lilin Feng,<sup>†a</sup> Liang Gao,<sup>†a</sup> Daniel F. Sauer,<sup>a</sup> Yu Ji,<sup>a</sup> Haiyang Cui,<sup>a</sup> and Ulrich Schwaneberg\*<sup>a,b</sup>

5 <sup>a</sup> Lehrstuhl für Biotechnologie, RWTH Aachen University, Worringerweg 3, 52074 Aachen, Germany

6 <sup>b</sup> DWI – Leibniz Institut für Interaktive Materialien, Forckenbeckstraße 50, 52074, Aachen, Germany

7 <sup>†</sup> These authors contributed equally to this work.

8 \*Corresponding author: Prof. Dr. Ulrich Schwaneberg

9 E-mail: [u.schwaneberg@biotec.rwth-aachen.de](mailto:u.schwaneberg@biotec.rwth-aachen.de)

10

11

12

13

14

15

16

17

18

19

20

21

22

23

24

25

26

27

28

29

30	<b>Experimental Procedures</b> .....	3
31	Chemicals.....	3
32	Cell culture.....	3
33	Immobilization of His <sub>6</sub> -tagged eGFP on <i>E. coli</i> cell surface mediated by metal ions.....	3
34	Immobilization of eGFP <sup>His</sup> on other bacteria cell surface mediated by Fe <sup>3+</sup> .....	3
35	Flow Cytometry Analysis.....	4
36	Metal absorption capacities of <i>E. coli</i> cells.....	4
37	Outer membrane fractionation.....	4
38	FITR analysis of <i>E. coli</i> BL21 whole cells and outer membrane fraction.....	4
39	Detachment test.....	5
40	1, 10-phenanthroline assay.....	5
41	Cell viability test of the Fe <sup>3+</sup> mediated immobilization method.....	5
42	Expression and purification of His <sub>6</sub> -tagged enzymes.....	6
43	Immobilization of His <sub>6</sub> -tagged enzymes on the cell surface mediated by Fe <sup>3+</sup> .....	6
44	Construction and expression of Strep-tag II_enzymes_His <sub>6</sub> -tag.....	7
45	Staining Strep-tag II with Strep-Tactin Chromeo™ 546 conjugate.....	7
46	Immobilization of multiple proteins on the cell surface through Fe <sup>3+</sup> .....	7
47	Construction of HRP-mCherry-His <sub>6</sub> tag.....	8
48	Expression and purification of HRP-mCherry-His <sub>6</sub> tag.....	8
49	Immobilization of HRP-mCherry <sup>His</sup> on the cell surface mediated by Fe <sup>3+</sup> .....	8
50	Modification of alginate with fluorescein and phenol group.....	8
51	Cell encapsulation in fluorescent alginate.....	9
52	<b>Supplementary results</b> .....	10
53	Supplementary Table 1: Metal ions adsorption after exogenous supplementation of different metal ions.....	10
54	Supplementary Figure 1: The effects of metal ions on the fluorescence of eGFP <sup>His</sup> .....	11
55	Supplementary Figure 2: Optimization and quantification of the immobilization method.....	12
56	Supplementary Figure 3: Cell-surface immobilization of eGFP <sup>His</sup> for <i>E. coli</i> K12, <i>Bacillus subtilis</i> and <i>Corynebacterium</i>	
57	<i>glutamicum</i> .....	14
58	Supplementary Figure 4: FTIR analysis of <i>E. coli</i> BL21 and the isolated outer membrane fraction.....	15
59	Supplementary Figure 5: The influence of L-ascorbic acid on eGFP <sup>His</sup> .....	16
60	Supplementary Figure 6: the immobilization of eGFP <sup>His</sup> on the cell surface while cell growth.....	17
61	Supplementary Figure 7: SDS-PAGE for the purified His <sub>6</sub> -tagged enzymes.....	18
62	Supplementary Figure 8: visualization of the His <sub>6</sub> -tagged enzymes on the cell surface.....	19
63	Supplementary Figure 9: Two proteins immobilized in the cell surface.....	20
64	Supplementary Figure 10: Modification of alginate with phenols and fluorophores (Fluor-Alg-Ph).....	21
65	Supplementary Figure 11: <sup>1</sup> H NMR spectroscopy of Fluor-Alg-Ph.....	22
66	Supplementary Figure 12: Immobilization of HRP-mCherry <sup>His</sup> on <i>E. coli</i> surface mediated by Fe <sup>3+</sup> .....	23
67	Supplementary Figure 13: Reaction scheme for hydrogel polymerization reaction initiated by HRP.....	24
68	Supplementary Figure 14: Fluorescence image of <i>E. coli</i> cells encapsulated in a conformal alginate shell.....	25
69	<b>Appendix</b> .....	26
70	<b>References</b> .....	27
71		

## 72 **Experimental Procedures**

### 73 **Chemicals**

74 All chemicals are of analytical grade or higher purity and were purchased from Merck  
75 (Darmstadt, Germany), AppliChem (Darmstadt, Germany), and Carl Roth (Karlsruhe, Germany)  
76 if not otherwise specified. The *E. coli* strains DH5 $\alpha$ , and BL21 Gold (DE3) were obtained from  
77 Agilent Technologies (Santa Clara, USA). The expression strain *Pichia pastoris* (*Komagataella*  
78 *phaffii*) BSYBG11 and plasmid pBSYA1S1Z were purchased from Bisy GmbH (Hofstätten/Raab,  
79 Austria).

### 80 **Cell culture**

81 *E. coli* BL21 Gold (DE3), *E. Coli* K12, and *Bacillus subtilis* were cultured at 37 °C, 250 rpm in  
82 Lysogeny Broth medium (5 g/L yeast extract, 10 g/L peptone, 10 g/L NaCl) overnight.  
83 *Corynebacterium glutamicum* was cultured at 30 °C, 250 rpm in BHI medium (37 g/L BHI  
84 powder, 10 g/L D-glucose) overnight. The cells were harvested and washed two times with  
85 0.9% (w/v) NaCl aqueous solution and stored in 0.9% (w/v) NaCl aqueous solution on ice prior  
86 to be used.

### 87 **Immobilization of His<sub>6</sub>-tagged eGFP on *E. coli* cell surface mediated by metal** 88 **ions**

89 The immobilization test of His<sub>6</sub>-tagged eGFP (eGFP<sup>His</sup>) on the *E. coli* cell surface was performed  
90 by addition of 100  $\mu$ M metal-chloride solution (*e.g.*, Fe<sup>3+</sup>, Ni<sup>2+</sup>, Co<sup>2+/3+</sup>, Cu<sup>2+</sup>, and Zn<sup>2+</sup>) and 5  
91  $\mu$ M eGFP<sup>His</sup> to the suspension of cells (0.9% (w/v) NaCl; OD<sub>600</sub> = 4) for 10 min at room  
92 temperature (total volume = 100  $\mu$ L). Then, the *E. coli* cells were collected by centrifugation  
93 at 11000 rpm for 1 min, washed with 100  $\mu$ L 0.9% (w/v) NaCl two times at room temperature  
94 resuspended in 100  $\mu$ L 0.9% (w/v) NaCl. A suspension of *E. coli* cells mixed with Fe<sup>3+</sup>/eGFP (no  
95 His<sub>6</sub>-Tag) or only eGFP<sup>His</sup> were used as controls, respectively. The fluorescence was detected  
96 *via* fluorescence microscope (Olympus Corporation, Japan) at the exposure time of 109.7 ms  
97 and the gain of 2.9 dB.

### 98 **Immobilization of eGFP<sup>His</sup> on other bacterial cell surface mediated by Fe<sup>3+</sup>**

99 For *E. coli* K12 and *Corynebacterium glutamicum*, the immobilization was performed according  
100 to the method mentioned above. For *Bacillus subtilis* cells, the immobilization was performed  
101 by addition of 300  $\mu$ M FeCl<sub>3</sub> (final concentration) into the cell suspension (0.9% (w/v) NaCl;

102 OD<sub>600</sub> = 4; total volume = 100 μL) for 10 min at room temperature followed by washing the  
103 cells one time with 0.9% (w/v) NaCl to remove unbound Fe<sup>3+</sup>. Afterwards, the cells were  
104 resuspended in 100 μL 0.9% (w/v) NaCl and mixed with 2 μL 250 μM eGFP<sup>His</sup> (final  
105 concentration 5 μM) for 5 min at room temperature. Finally, the *Bacillus* cells were harvested  
106 by centrifugation at 8000 rpm for 2 min, washed with 0.9% (w/v) NaCl two times at room  
107 temperature, and resuspended in 0.9% (w/v) NaCl. The suspensions of these bacteria cells  
108 mixed with Fe<sup>3+</sup>/eGFP (no His<sub>6</sub>-Tag) or only eGFP<sup>His</sup> were used as controls. The fluorescence  
109 was analyzed via fluorescence microscope (Olympus Corporation, Japan) at the exposure time  
110 of 109.7 ms and the gain of 2.9 dB.

### 111 **Flow Cytometry Analysis**

112 Single cell immobilization efficiency was detected by transferring the resulting cell  
113 suspensions (in 0.9% (w/v) NaCl) to polystyrene tubes for flow cytometry analysis (BD Influx™,  
114 USA). The population of cells was gated based on forward and side scatter emission, and the  
115 eGFP signal was determined by fluorescence intensity on the 488/30 BP Filter emission  
116 channel.

### 117 **Metal absorption capacities of *E. coli* cells**

118 5 mL of *E. coli* cells (OD<sub>600</sub> = 4) were resuspended in 0.9% (w/v) NaCl and then supplemented  
119 with 100 μM of FeCl<sub>3</sub>, ZnCl<sub>2</sub>, CuCl<sub>2</sub>, NiCl<sub>2</sub>, and CoCl<sub>2</sub>. After 10 min, the cells were washed two  
120 times with 5 mL 0.9% (w/v) NaCl, and then the pellets were collected. The resulting pellets  
121 were incubated overnight in 5 mL 70% nitric acid (22.22 M) at 50 °C. Metal contents of these  
122 samples was determined by atomic emission spectroscopy (ICP-OAS) (PlasmaQuant PQ9000  
123 Elite, Analytik Jena) <sup>1</sup>.

### 124 **Outer membrane fractionation**

125 *E. coli* cells grown overnight at 37 °C were collected and suspended in 0.9 % (w/v) NaCl (OD<sub>600</sub>  
126 of 4.0; total volume = 200 mL). The suspensions, containing 50 μg/mL of deoxyribonuclease  
127 and 100 μg/mL of ribonuclease, were then passed through French press to lyse the cells. The  
128 cell lysates were centrifuged at 5,000 g (4 °C, 1 h). The resulting pellets were resuspended in  
129 0.9 % (w/v) NaCl supplemented with 2% (v/v) Triton X-100 and incubated at room temperature  
130 for 30 min. The suspension was subsequently centrifuged at 100,000 g (4 °C, 30 min). The

131 resulting pellet contained the outer membrane fraction was dried by lyophilization for two  
132 days prior to FTIR analysis. This method is based on a protocol developed by Beveridge et al.<sup>2</sup>

### 133 **FTIR analysis of *E. coli* BL21 whole cells and outer membrane fraction**

134 The FTIR was performed with a FTIR spectrometer (Avatar Nicolet 360 FT-IR, ThermoFisher,  
135 USA). 5 mg of dried outer membrane fraction was mixed with 150 mg of KBr (Spectral) in an  
136 agate mortar. The translucent discs were prepared by pressing the KBr mixture with the aid of  
137 10 t pressure bench press. The disc was immediately analyzed using a spectrophotometer in  
138 the range of 4000-400 cm<sup>-1</sup>. Atmospheric water and CO<sub>2</sub> were subtracted.

### 139 **Detachment test**

140 Detachment test of eGFP<sup>His</sup> on the cell surface was carried out by using L-ascorbic acid to  
141 reduce Fe<sup>3+</sup> to Fe<sup>2+</sup>. 100 μL cell suspension with immobilized eGFP<sup>His</sup> (0.9% (w/v) NaCl; OD<sub>600</sub> =  
142 4) was incubated with L-ascorbic acid (250 μM) for 30 min at room temperature. Afterwards  
143 the cells were washed twice with 100μL 0.9% (w/v) NaCl and resuspended in 100μL 0.9% (w/v)  
144 NaCl. Cell-surface immobilized eGFP<sup>His</sup> without addition of L-ascorbic acid served as control.  
145 The influence of L-ascorbic acid on the fluorescence of eGFP was investigated by  
146 supplementing 250 μM L-ascorbic acid to 100 μL solution containing 5 μM eGFP<sup>His</sup> for 100 min  
147 at room temperature. eGFP<sup>His</sup> without L-ascorbic acid was used as control. Fluorescence was  
148 detected *via* Tecan Infinite M1000 Pro plate reader (Tecan Group, Mannedorf, Switzerland;  
149 λ<sub>ex</sub> = 488 nm and λ<sub>em</sub> = 507 nm).

### 150 **1, 10-phenanthroline assay**

151 The cell surface reduced Fe<sup>2+</sup> was measured through 1,10-phenanthroline assay (Fe<sup>2+</sup> form a  
152 deep red solution with 1,10-phenanthroline)<sup>2</sup>. After the eGFP<sup>His</sup> detachment procedure, 400  
153 μL resulting cells suspension was added to 150 μL 1,10-phenanthroline solutions (5 mM).  
154 Subsequently, 450 μL sodium acetate buffer (200 mM, pH 4.5) was added, and the mixture  
155 was incubated for 10 min at room temperature. Fe<sup>3+</sup> decorated cells without L-ascorbic acid  
156 were used as control.

### 157 **Cell viability test of the Fe<sup>3+</sup> mediated immobilization method**

158 After immobilization, the cell viability was determined by adding 5 μL cell suspension into 195  
159 μL LB<sub>Kan</sub> medium in the microtiter plate. The cell OD<sub>600</sub> was measured by Tecan Sunrise™ plate  
160 reader (Tecan Group, Mannedorf, Switzerland; 600 nm). After 30 min and 60 min of culture,

161 5  $\mu$ L of the cultures were taken out for the fluorescence microscope detection, respectively.  
162 The cells without immobilization were used as control.

### 163 **Expression and purification of His<sub>6</sub>-tagged enzymes**

164 Cloning and expression of His<sub>6</sub>-tagged *Bacillus licheniformis* laccase (BlcotA<sup>His</sup>)<sup>3</sup>, His<sub>6</sub>-tagged  
165 *Bacillus subtilis* lipase A (BSLA<sup>His</sup>)<sup>4</sup>, and His<sub>6</sub>-tagged *Candida tropicalis* fatty alcohol oxidase  
166 (CtFAO<sup>His</sup>)<sup>5</sup> were performed according to the published procedures. After expression, cells  
167 were harvested by centrifugation at 4,000 rpm for 15 minutes then resuspended in 20 mL  
168 optimal buffer (according to the enzymes) containing 150 mM NaCl, 10 mM imidazole. Cells  
169 were disrupted by sonication and debris removed by centrifugation at 15,000  $\times$  g for 1 hour  
170 (Sorvall, ThermoFischer Scientific, Germany). The supernatant was then applied to the  
171 Protino1 Ni-TED 2,000 packed columns (Macherey-Nagel). Afterwards, PD-10 desalting  
172 column (GE Healthcare, Germany) was used to remove salts. The purified lipases were stored  
173 at glycine buffer (10 mM, pH 10.5) in small aliquots at -80 °C, and each aliquot was used only  
174 once after thawing. Purity was determined using the Experion<sup>TM</sup> system from Bio-Rad  
175 (München, Germany).

### 176 **Immobilization of His<sub>6</sub>-tagged enzymes on the cell surface mediated by Fe<sup>3+</sup>**

177 Immobilization of His<sub>6</sub>-tagged enzymes on the cell surface was performed by adding FeCl<sub>3</sub> (0;  
178 50; 100  $\mu$ M, respectively) and 1  $\mu$ M His<sub>6</sub>-Tag enzymes to *E. coli* cell suspensions (0.9% (w/v)  
179 NaCl; OD600 = 4; total volume = 100  $\mu$ L). The solution was incubated for 10 min at room  
180 temperature, and then the cells were washed two times and resuspended with 100  $\mu$ L 0.9%  
181 (w/v) NaCl. The activity of BlcotA<sup>His</sup> and CtFAO<sup>His</sup> on the cell surface were detected via ABTS  
182 assay, 30  $\mu$ L cell suspension was added into 170  $\mu$ L ABTS mix solution (3 mM in 100 mM HAC-  
183 NaAc buffer, pH 4.5 for BlcotA<sup>His</sup>; 50 mM KPi buffer, pH 7.4 for CtFAO<sup>His</sup>). The increase in  
184 absorbance was measured at 420 nm for 20 min via Tecan Sunrise<sup>TM</sup> plate reader. The activity  
185 of BSLA<sup>His</sup> on the cell surface was detected via *p*-nitrophenyl butyrate (*p*NBP) assay. *p*NBP  
186 stock solution (10 mM in acetonitrile) was prepared in advance, and then the master mix  
187 solution was prepared by adding 9 mL TEA buffer (Triethanolamin, pH 7.4) to 1 mL *p*NBP stock  
188 solution. The measurement was initiated by adding 50  $\mu$ L cells suspension to 150  $\mu$ L master  
189 mix solution, and then the absorbance was measured at 410 nm for 20 min via Tecan Sunrise<sup>TM</sup>  
190 plate reader.

## 191 **Construction and expression of Strep-tag II\_enzymes\_His<sub>6</sub>-tag**

192 Strep-tag II (eight amino acids: **WSHPQFEK**) was introduced into the *N*-terminus of each  
193 protein as **5'-ASA-strep-tag II-SG-BlcotA\_His<sub>6</sub>-tag-3'** (**StrepII\_BlcotA<sup>His</sup>**), **5'-ASA-strep-tag II-**  
194 **SG-BSLA\_His<sub>6</sub>-tag-3'** (**StrepII\_BSLA<sup>His</sup>**) and **5'-ASA-strep-tag II-SG-CtFAO\_His<sub>6</sub>-tag-3'**  
195 (**StrepII\_CtFAO<sup>His</sup>**). The protein expression and purification were performed according to the  
196 protocol mentioned above.

## 197 **Staining Strep-tag II with Strep-Tactin Chromeo™ 546 conjugate**

198 After immobilization (according to the method mentioned above), 2 μL Strep-Tactin  
199 Chromeo™ 546 conjugate (0.5 mg/ml solution in PBS, 10 × dilute before usage, IBA  
200 Lifesciences, Göttingen, DE) was added into 50 μL of cell suspension immobilized with  
201 StrepII\_enzymes\_His<sub>6</sub>-tag (0.9% (w/v) NaCl; OD<sub>600</sub> = 4). The mixture was incubated at room  
202 temperature with 900 rpm shaking for 15 min, and then cells were washed twice and  
203 resuspended in 50 μL 0.9% (w/v) NaCl. Afterwards, cells were analyzed by fluorescence  
204 microscopy ( $\lambda_{\text{ex}} = 555 \text{ nm}$ ;  $\lambda_{\text{em}} = 640 \text{ nm}$ ). To analyze the conjugation of the immobilized  
205 enzymes in different buffers, 30 μL of cell suspension immobilized with StrepII\_BlcotA<sup>His</sup> or  
206 StrepII\_CtFAO<sup>His</sup> were transferred into 170 μL ABTS mix solution (100 mM HAc-NaAc buffer,  
207 pH 4.5 and 50 mM KPi buffer, pH 7.4; respectively) for 30 min at room temperature; 50 μL of  
208 cell suspensions immobilized with StrepII\_BSLA<sup>His</sup> were transferred into 150 μL pNBP master  
209 mix solution (50 mM TEA buffer, pH 7.4)) for 30 min at room temperature. After incubation,  
210 the cells were washed twice and resuspended in 50 μL 0.9% (w/v) NaCl. The following staining  
211 step was performed as described above. The resulting cells were analyzed by fluorescence  
212 microscopy ( $\lambda_{\text{ex}} = 555 \text{ nm}$ ;  $\lambda_{\text{em}} = 640 \text{ nm}$ ).

## 213 **Immobilization of multiple proteins on the cell surface through Fe<sup>3+</sup>**

214 StrepII\_BlcotA<sup>His</sup> and eGFP<sup>His</sup> were used to perform the cell surface immobilization of different  
215 proteins. To this end, 40 μM StrepII\_BlcotA<sup>His</sup> and 40 μM eGFP<sup>His</sup> were mixed. 10 μL mixture  
216 was then add to 100 μL cell suspension supplied with 100 μM FeCl<sub>3</sub> (0.9% (w/v) NaCl; OD<sub>600</sub> =  
217 4). After washing the cells twice, the cells were resuspended in 0.9% (w/v) NaCl. The  
218 immobilization of StrepII\_BlcotA<sup>His</sup> was visualized by staining the StrepII tag with Strep-Tactin  
219 conjugated Chromeo™ 546 (the details were shown above). The fluorescence was detected  
220 via fluorescence microscope (Olympus Corporation, Japan) at the exposure time of 109.7 ms  
221 and the gain of 2.9 dB.

## 222 **Construction of HRP-mCherry-His<sub>6</sub> tag**

223 Horseradish peroxidase (HRP, EC 1.11.1.7, Genebank accession: AIV09214.1) from *Armoracia*  
224 *rusticana*<sup>6</sup> was synthesized by GeneScript with codon optimization for *Pichia pastoris*  
225 BSYBG11. HRP gene was then cloned and fused to the *N*-terminus of mCherry (red  
226 fluorescence protein) with a flexible linker GGGs as shown as 5'-HRP-GGGs-mCherry-His<sub>6</sub> tag-  
227 3'. The whole construct was inserted into pBSYA1S1Z plasmid and then transformed into  
228 chemical-competent *E. coli* BL21 DH5 $\alpha$ . The resulting plasmid, pBSYA1S1Z-HRP-mCherry-His<sub>6</sub>  
229 tag, was isolated and transformed into *Pichia pastoris* BSYBG11 via electroporation.

## 230 **Expression and purification of HRP-mCherry-His<sub>6</sub> tag**

231 HRP-mCherry-His<sub>6</sub> tag (HRP-mCherry<sup>His</sup>) was overexpressed in *Pichia pastoris* BSYBG11. The  
232 pre-cultures were grown in 10 mL YPD medium (10 g/L yeast extract, 20 g/L peptone, 20 g/L  
233 D-glucose, 100 $\mu$ g/mL zeocin) using a 100 mL flask (30 °C, 200 rpm). Main cultures were  
234 inoculated using the pre-cultures as inoculum to a start OD<sub>600</sub> = 0.5 in 200 mL YPD medium.  
235 After cultivation (30 °C, 200 rpm), the culture supernatant was separated from the cell broth  
236 by centrifuging (Sorvall, ThermoFischer Scientific, Germany, 4 °C, 4000  $\times$  g, 30 min). Culture  
237 supernatant was concentrated 10 folds using an Amicon Ultra-15 Centrifugal Filter Unit (Merck  
238 Millipore Ltd. Tullagreen, Ireland; Cut off: 10 kDa). HRP-mCherry<sup>His</sup> was purified by using a Ni-  
239 IDA 2000 column. Samples eluted with 50 mM imidazole are dialyzed and stored in 0.9% (w/v)  
240 NaCl solution at -80 °C for further application.

## 241 **Immobilization of HRP-mCherry<sup>His</sup> on the cell surface mediated by Fe<sup>3+</sup>**

242 HRP-mCherry<sup>His</sup> (0.06 mg/mL) and different concentration of FeCl<sub>3</sub> (0; 30; 50  $\mu$ M) were added  
243 into 100 $\mu$ l fresh suspension of *E. coli* cells (0.9% (w/v) NaCl; OD<sub>600</sub> = 4) for 10 min at room  
244 temperature. After two times washing with 100 $\mu$ l 0.9% (w/v) NaCl, the resulting cells were  
245 examined by fluorescence microscope ( $\lambda_{ex}$  = 555 nm;  $\lambda_{em}$  = 640 nm) and ABTS colorimetric  
246 assay (details were shown above).

## 247 **Modification of alginate with fluorescein and phenol group**

248 The alginate with fluorescein and phenol group (Fluor-Alg-Ph) was prepared based on  
249 previously reported<sup>7,8</sup>. Briefly, sodium alginate was dissolved in the 50 mM MES buffer (pH  
250 6) with a concentration of 10 g/L. Then, 40 mM Tyramine hydrochloride, 10 mM *N*-  
251 hydroxysuccinimide (NHS), and 20 mM 1-ethyl-3-(3 dimethyl aminopropyl) carbodiimide-



252 hydrochloride (EDC) were added, respectively. The mixture was under continuous stirring by  
253 adding 2 mM 5-aminofluorescein (144 mM stock in DMSO) at room temperature for  
254 overnight. The modified polymer was precipitated with 80% cooled ethanol solution and  
255 collected by centrifugation (4000 × g, 4 °C for 10 min). The pellet was washed twice with 80%  
256 ethanol and then dissolved in water for lyophilization. The modified alginate was analyzed by  
257 <sup>1</sup>H-NMR (nuclear magnetic resonance, 300 MHz, 23 °C) in D<sub>2</sub>O.

### 258 **Cell encapsulation in fluorescent alginate**

259 In case of single cell encapsulation based on Fluor-Alg-Ph polymer, HRP-mCherry<sup>His</sup>  
260 immobilized *E. coli* cells (100 μL, OD<sub>600</sub> = 4) are harvested and resuspended in 1% (w/v) Fluor-  
261 Alg-Ph solution (100 μL, 0.9% (w/v) NaCl) containing 1 mM H<sub>2</sub>O<sub>2</sub>. The whole mixture was  
262 incubated at room temperature for 10 min and then harvested (11000 rpm, 2 min) and  
263 washed with 100 μL 0.9% (w/v) NaCl aqueous solution four times. The resuspended samples  
264 were transferred to fluorescence microscope for checking hydrogel formation ( $\lambda_{ex}=470$  nm,  
265  $\lambda_{em}=535$  nm).

266

267

268

269

270

271

272

273

274

275

276

277

278 **Supplementary results**

279 **Supplementary Table 1: Metal ions adsorption after exogenous**  
280 **supplementation of different metal ions**

281 *E. coli* cells retained 3.05 mg/g<sub>cells</sub> of Fe<sup>3+</sup> compared to the other probed metals. The metal  
282 absorption analysis explains to some extent the reason why other metal ions (e.g., Ni<sup>2+</sup>, Co<sup>2+</sup>,  
283 and Zn<sup>2+</sup>) with high His<sub>6</sub>-tagged affinity show no detectable immobilization ability of eGFP<sup>His</sup>.  
284 Notably, *E. coli* BL21 cells also exhibited high adsorption capacity towards Cu<sup>2+</sup>. However, in  
285 contrast to the fluorescence results obtained with Fe<sup>3+</sup>, the low labeling ability can be  
286 explained by non-optimal binding conditions of Cu<sup>2+</sup> towards the His<sub>6</sub>-tagged<sup>9</sup>.

287 **Table S1: Metal ions adsorption by *E. coli* cells**

	Metal ions absorbed (mg/g <sub>cells</sub> )				
	Fe <sup>3+</sup>	Zn <sup>2+</sup>	Cu <sup>2+</sup>	Ni <sup>2+</sup>	Co <sup>2+</sup>
<i>E. coli</i> BL21	0.09	0.06	< 0.02	<< 0.01	0.0
<i>E. coli</i> BL21 + Metal ions	3.05	0.84	2.79	0.31	0.11

288 5 mL of Cells (OD<sub>600</sub> = 4) were resuspended in 0.9% (w/v) NaCl and then supplemented with 100 μM of FeCl<sub>3</sub>,  
289 ZnCl<sub>2</sub>, CuCl<sub>2</sub>, NiCl<sub>2</sub>, and CoCl<sub>2</sub>, respectively. After 10 min, cells were washed twice with 0.9% (w/v) NaCl and then  
290 the pellets were collected. The resulting pellets were incubated overnight in 70% nitric acid (22.22 M) at 50°C.  
291 Metal content of these samples was determined by ICP-OAS.

292

293

294

295

296

297

298

299

300

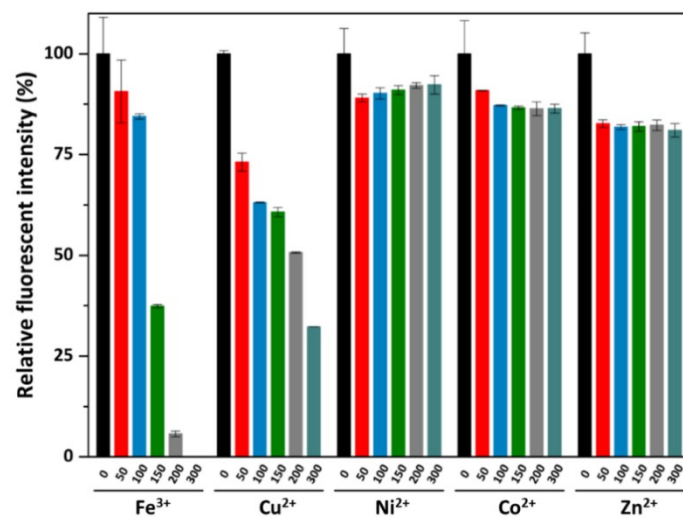
301

302

303

304 **Supplementary Figure 1: The effects of metal ions on the fluorescence of**  
305 **eGFP<sup>His</sup>**

306 The effect of metal ions on the fluorescence of eGFP<sup>His</sup> was examined. For Fe<sup>3+</sup>, metal  
307 concentrations below 100 μM showed a slight quenching effect on eGFP, but when the  
308 concentration was increased above 150 μM, the fluorescence of eGFP was strongly  
309 suppressed. For Cu<sup>2+</sup>, low concentrations of metal ions already have caused about 40% loss of  
310 eGFP fluorescence. The other tested metal ions (Ni<sup>2+</sup>; Co<sup>2+</sup>; Zn<sup>2+</sup>) have only a negligible effect  
311 on the fluorescence of eGFP.



312

313 **Figure S1:** The metal ions were incubated with 5 μM eGFP<sup>His</sup> for 10 min, and then the residual fluorescence  
314 intensity was measured at λ<sub>ex</sub> = 488 nm; λ<sub>em</sub> = 507 nm. For each metal ions, six different concentrations were  
315 tested (0; 50; 100; 150; 200; 300 mM). Error bars indicate standard deviations of two technical replicates.

316

317

318

319

320

321

322

323

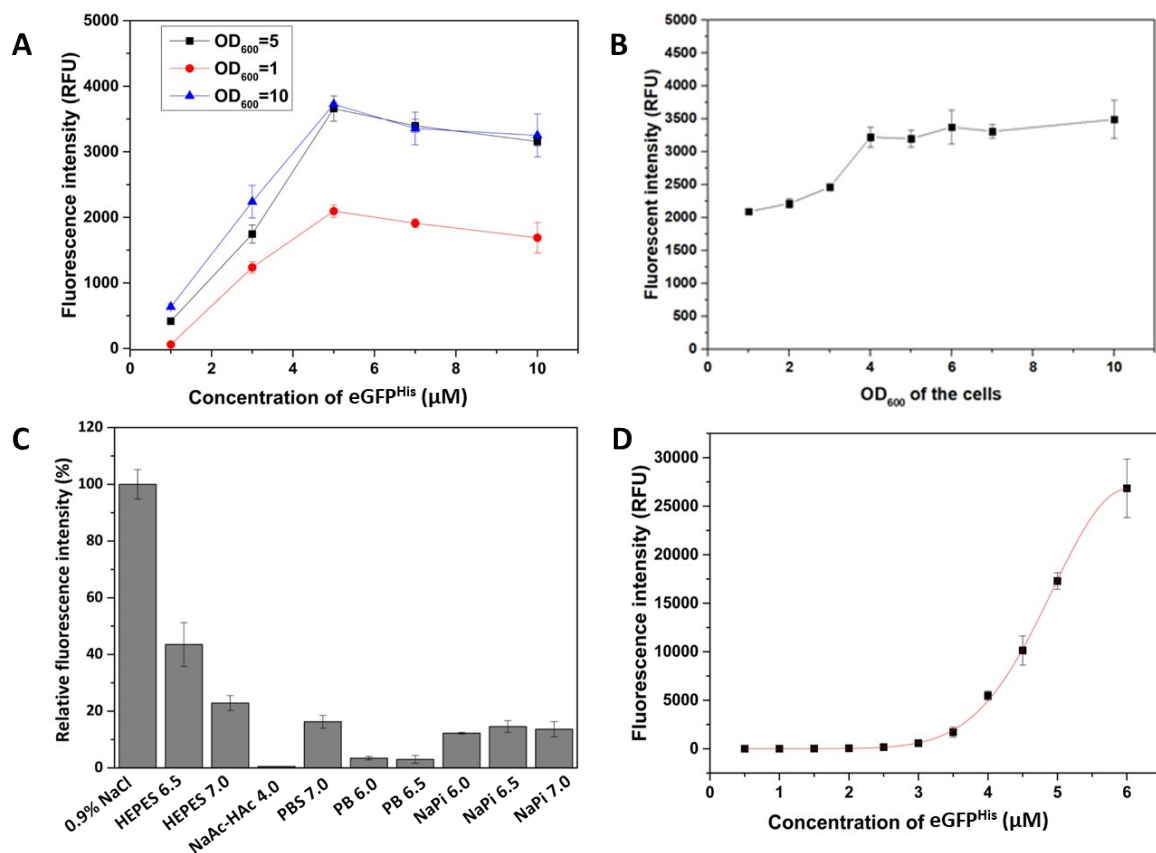
324

325

326

327 **Supplementary Figure 2: Optimization and quantification of the immobilization**  
 328 **method**

329 The immobilization conditions were optimized. Firstly, we tested the saturation concentration  
 330 of eGFP<sup>His</sup> for 100 μM Fe<sup>3+</sup>. The highest fluorescence intensity was reached at 5 μM eGFP<sup>His</sup>,  
 331 despite testing the number of cells (Figure S2A). Then under this concentration of eGFP<sup>His</sup>, the  
 332 optimal cell concentration was measured utilizing 100 μM Fe<sup>3+</sup>. It was shown that when cell  
 333 OD<sub>600</sub> is 4, the fluorescence intensity reached highest and no obvious fluorescence increased  
 334 by adding more cells. It indicated 100 μM Fe<sup>3+</sup> realized saturation at cell OD<sub>600</sub> = 4 (Figure S2B).  
 335 Additionally, the buffer system was optimized (Figure S2C). It was shown that the best working  
 336 solution for immobilization is 0.9 % (w/v) NaCl. Hence, the optimal condition was determined  
 337 that 100 μM Fe<sup>3+</sup> and 5 μM eGFP<sup>His</sup> are add to the *E. coli* cells (suspend in 0.9% (w/v) NaCl;  
 338 OD<sub>600</sub> = 4). Under this optimal condition, it can be calculated that 100 μM Fe<sup>3+</sup> could mediate  
 339 around 3.82 μM eGFP<sup>His</sup> immobilized on the cell surface when the cell OD<sub>600</sub> is 4, comparing  
 340 with the calibration curve ( $y = \exp^{100x}(-4.8003 + 4.98x - 0.413x^2)$ ; R<sup>2</sup> = 0.997) (Figure S2D).



341

342 **Figure S2:** (A) Saturation line of 100 μM Fe<sup>3+</sup> for different concentration eGFP<sup>His</sup>. 100 μM Fe<sup>3+</sup> and different  
 343 concentration of eGFP<sup>His</sup> were added to the suspension of *E. coli* cells (0.9% (w/v) NaCl). Red line: cell suspension

344 at  $OD_{600} = 1$ ; black line: cell suspension at  $OD_{600} = 5$ ; blue line: cell suspension at  $OD_{600} = 10$ . (B) Saturation line of  
345  $100 \mu\text{M Fe}^{3+}$  for different cell density ( $OD_{600}$ ).  $100 \mu\text{M Fe}^{3+}$  and  $5 \mu\text{M eGFP}^{\text{His}}$  were added to the suspension of *E.*  
346 *coli* cells (0.9% (w/v) NaCl), whereas the concentration of cells was varied. (C) Cell binding of  $e\text{GFP}^{\text{His}}$  in different  
347 solutions. The fluorescence intensity of immobilized  $e\text{GFP}^{\text{His}}$  was measured at  $\lambda_{\text{ex}} = 470 \text{ nm}$ ;  $\lambda_{\text{em}} = 535 \text{ nm}$ . Error  
348 bars indicate standard deviations of two technical replicates. (D) Calibration curves of  $e\text{GFP}^{\text{His}}$  under  $100 \mu\text{M Fe}^{3+}$ .  
349 Different concentration of  $e\text{GFP}^{\text{His}}$  was incubate with  $100 \mu\text{M Fe}^{3+}$  for 10 min at room temperature.

350

351

352

353

354

355

356

357

358

359

360

361

362

363

364

365

366

367

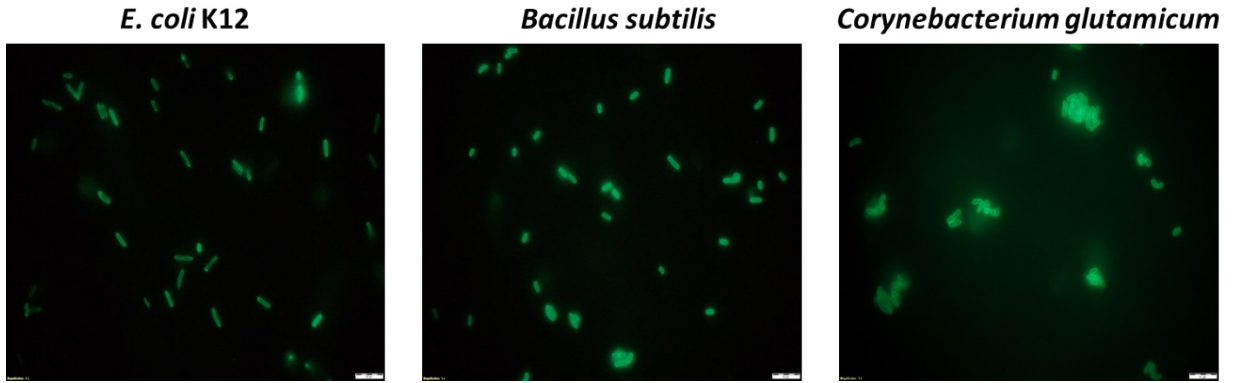
368

369

370

371 **Supplementary Figure 3: Cell-surface immobilization of eGFP<sup>His</sup> for *E. coli***  
372 ***K12, Bacillus subtilis* and *Corynebacterium glutamicum***

373



374

375 **Figure S3:** Fluorescence image of the cell surface of different strains immobilized with eGFP<sup>His</sup>.

376

377

378

379

380

381

382

383

384

385

386

387

388

389

390

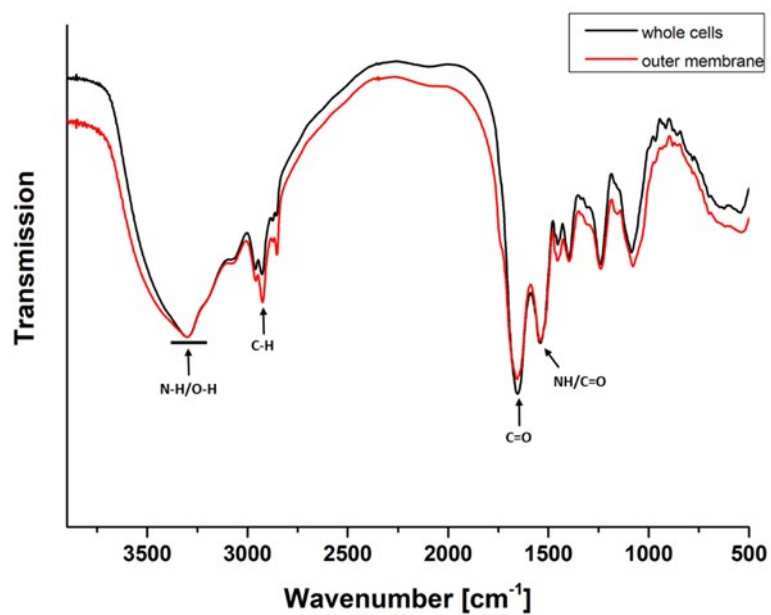
391

392

393 **Supplementary Figure 4: FTIR analysis of *E. coli* BL21 and the isolated outer**  
394 **membrane fraction**

395 FTIR spectra of *E. coli* BL21 and its isolated outer membrane fraction, in the range of 4000 -  
396 500  $\text{cm}^{-1}$ , were taken to confirm the presence of functional groups (Fig. S4). FTIR suggests  
397 that carbonyl groups belonging to carboxylic acids or amides as well as free amines are present  
398 for metal coordination.

399



400

401 **Figure S4:** FTIR spectra of *E. coli* BL21 whole cells (black line) and outer membrane fraction of *E. coli* BL21 (red  
402 line).

403

404

405

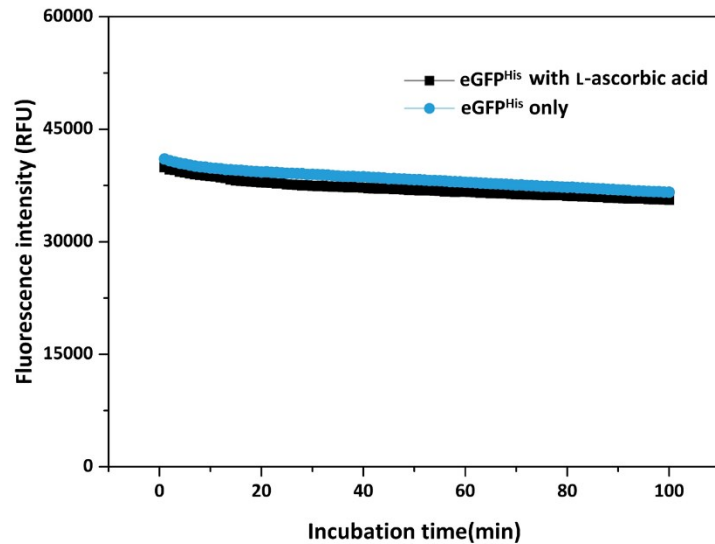
406

407

408

409 **Supplementary Figure 5: The influence of L-ascorbic acid on eGFP<sup>His</sup>**

410 The time-dependent fluorescence curve shows that L-ascorbic acid has no effect on the  
411 fluorescence of eGFP<sup>His</sup> (Figure S5).



412

413 **Figure S5:** Time-dependent fluorescence curve of the influence of L-ascorbic acid on the fluorescence of eGFP<sup>His</sup>.

414 Black line: 250  $\mu$ M L-ascorbic acid was added to 5  $\mu$ M eGFP<sup>His</sup> for 100 min; blue line: only 5  $\mu$ M eGFP<sup>His</sup> was  
415 incubated for 100 min. The fluorescence intensity was measured by Tecan Infinite M1000 Pro plate reader ( $\lambda_{\text{ex}}$  =  
416 488 nm;  $\lambda_{\text{em}}$  = 507 nm).

417

418

419

420

421

422

423

424

425

426

427

428

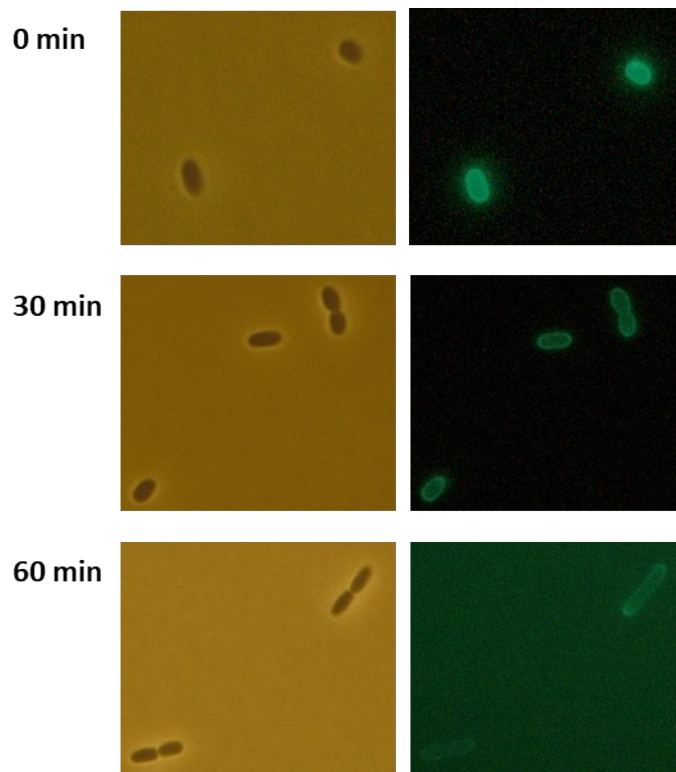
429

430



431 **Supplementary Figure 6: the immobilization of eGFP<sup>His</sup> on the cell surface while**  
432 **cell growth**

433 During cell growth, the immobilization of eGFP<sup>His</sup> on the cell surface was inspected by  
434 fluorescence microscopy. As shown in Figure S6, after 30 min and 60 min culture, eGFP<sup>His</sup>  
435 remained on the cell. During cell growth, the cell-mass increases, which leads to reduced  
436 fluorescence intensity, since the total amount of eGFP is constant. For applications, either the  
437 cells need to be kept in the static phase or new Fe<sup>3+</sup>/His<sub>6</sub>-tagged protein need to be  
438 supplemented to ensure homogeneous distribution of the protein on the cell surface.



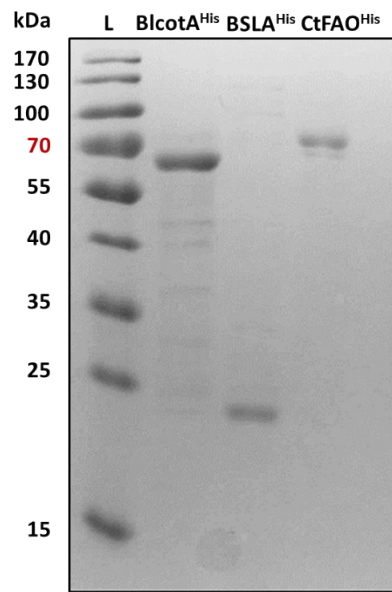
439

440 **Figure S6:** Fluorescence images of eGFP<sup>His</sup> immobilized on the cell surface during cell growth. The image was  
441 inspected by fluorescence microscope in bright and green fields ( $\lambda_{\text{ex}} = 470 \text{ nm}$ ,  $\lambda_{\text{em}} = 535 \text{ nm}$ ) at the exposure  
442 time of 109.7 ms and the gain of 2.9 dB.

443

444

445 **Supplementary Figure 7: SDS-PAGE for the purified His<sub>6</sub>-tagged enzymes**



446

447 **Figure S7:** SDS-PAGE of purified BlcotA<sup>His</sup>, BSLA<sup>His</sup>, and CtFAO<sup>His</sup>. The molecular weight of each protein is 60.4,  
448 19.3, 78 kDa, respectively. L: Ladder (PageRuler™ Prestained Protein Ladder (Thermo Scientific)).

449

450

451

452

453

454

455

456

457

458

459

460

461

462

463

464

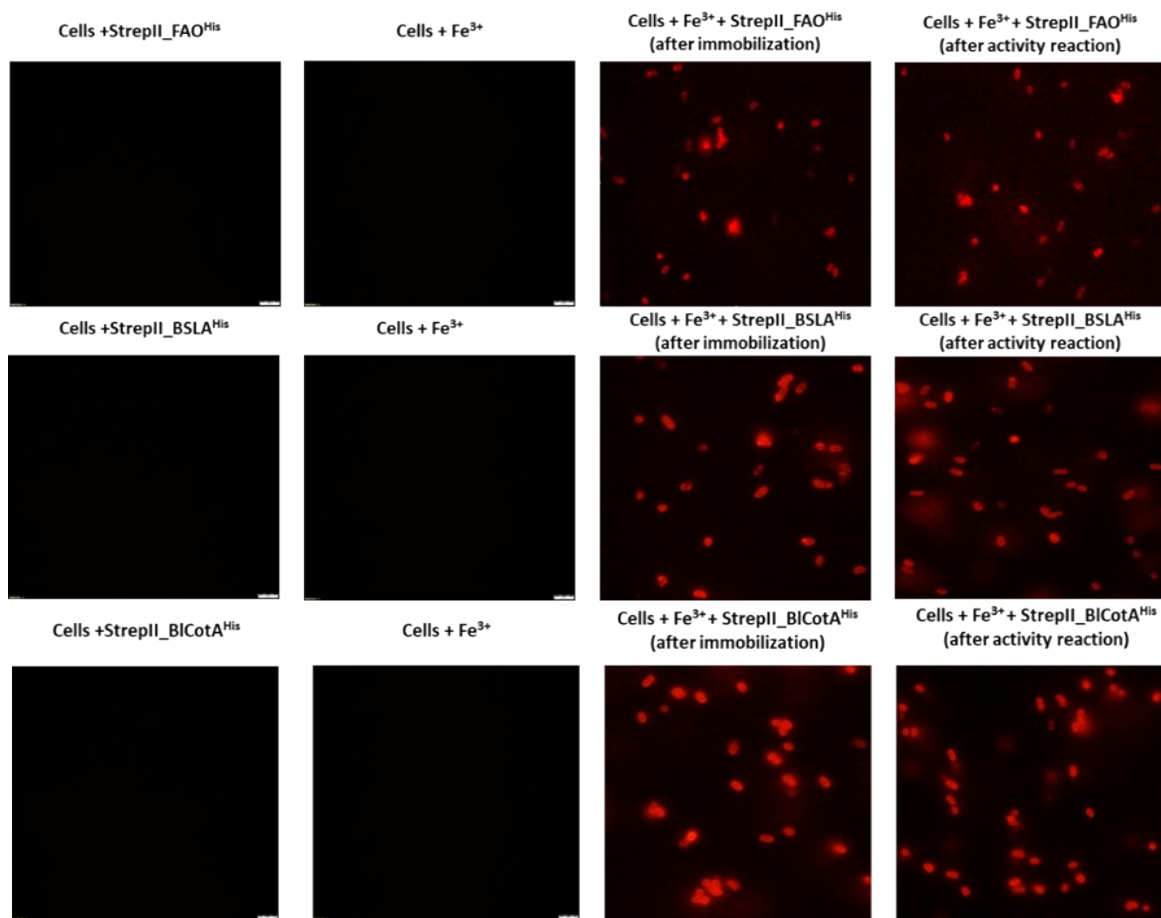
465

466

467

468 **Supplementary Figure 8: visualization of the His<sub>6</sub>-tagged enzymes on the cell**  
469 **surface**

470 Direct visualization of the His<sub>6</sub>-tagged enzymes on the cell surface was performed by Strep-  
471 tag II, which can combine with Strep-Tactin conjugated fluorophore (Chromeo™ 546).  
472 Fluorescence microscopy revealed that the His<sub>6</sub>-tagged enzymes successfully remained on the  
473 cell surface after immobilization and their corresponding activity assay, which was performed  
474 in a different buffer.



475

476 **Figure S8:** Fluorescence images of cells immobilized with Strep-tag II\_enzymes\_His<sub>6</sub>-tag after staining with Strep-  
477 Tactin Chromeo™ 546 conjugate. The red fluorescence signal (Chromeo™ 546) directly indicated the His<sub>6</sub>-tagged  
478 enzymes are successfully immobilized on the cell surface before and after activity assay reaction. The image was  
479 inspected by fluorescence microscope in red fields ( $\lambda_{ex}$  = 555 nm;  $\lambda_{em}$  = 640 nm) at the exposure time of 109.7 ms  
480 and the gain of 2.9 dB.

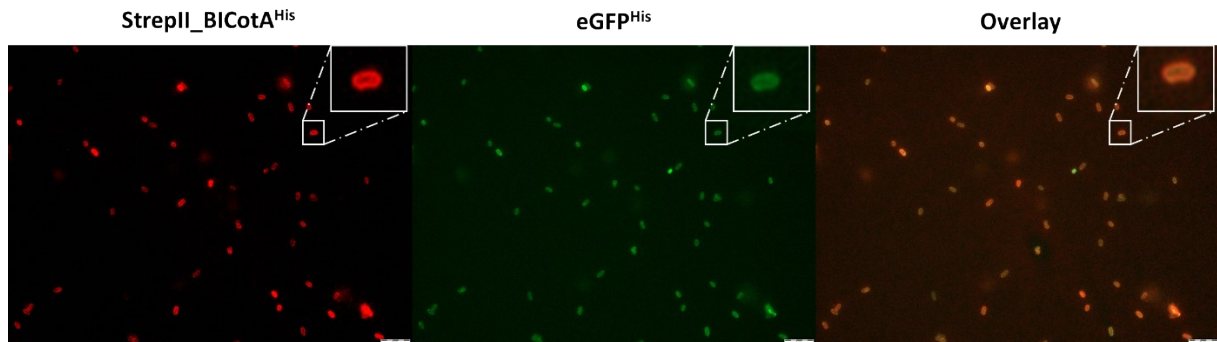
481

482

483

484 **Supplementary Figure 9: Two proteins immobilized in the cell surface**

485 The images of fluorescence microscopy confirms that both proteins, StrepII\_BICotA<sup>His</sup> and  
486 eGFP<sup>His</sup>, are presented on *E. coli* cells.



487

488 **Figure S9:** Fluorescence images of cells immobilized with StrepII\_BICotA<sup>His</sup> and eGFP<sup>His</sup>. The immobilization of  
489 StrepII\_BlcotA<sup>His</sup> was visualized by staining the Strep tag II with Strep-Tactin conjugated Chromeo™ 546. The cells  
490 were inspected by fluorescence microscopy in green field ( $\lambda_{ex} = 470$  nm,  $\lambda_{em} = 535$  nm) and red field ( $\lambda_{ex} = 555$   
491 nm;  $\lambda_{em} = 640$  nm) at the exposure time of 109.7 ms and the gain of 2.9 dB.

492

493

494

495

496

497

498

499

500

501

502

503

504

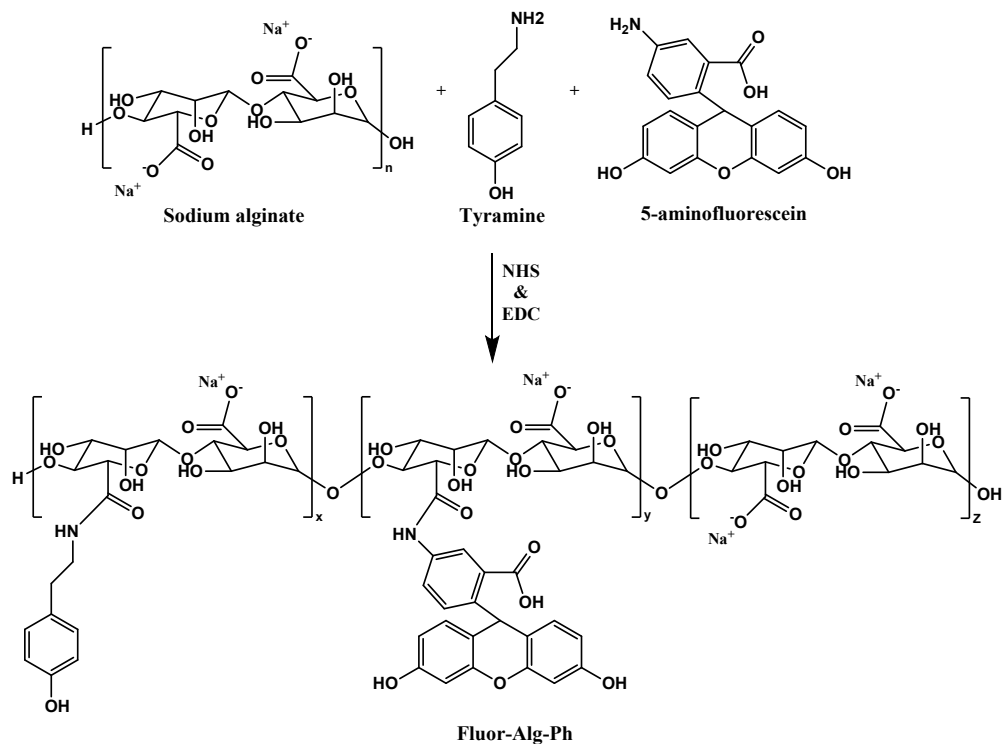
505

506

507

508 **Supplementary Figure 10: Modification of alginate with phenols and**  
509 **fluorophores (Fluor-Alg-Ph)**

510



511

512 **Figure S10:** Reaction scheme for the production of alginate macromonomers (Fluor-Alg-Ph).

513

514

515

516

517

518

519

520

521

522

523

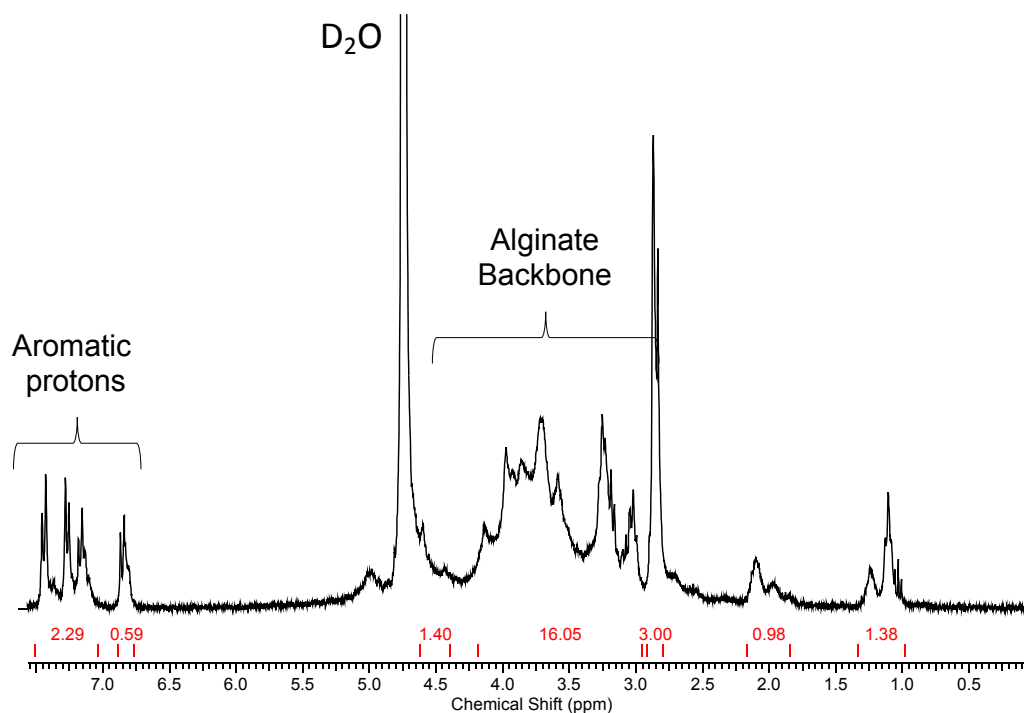
524

525

526

527 **Supplementary Figure 11:  $^1\text{H}$  NMR spectroscopy of Fluor-Alg-Ph**

528  $^1\text{H}$  NMR spectra were recorded on a Bruker Avance III 300 MHz NMR spectrometer (Bruker,  
529 Massachusetts). Deuterium oxide ( $\text{D}_2\text{O}$ ) was used as NMR solvent and the NMR signals are  
530 reported relative to the remaining proteo solvent at 4.75 ppm<sup>10</sup>. The signals above  $\delta = 6.8$   
531 ppm indicate the aromatic moieties attached upon the EDC/NHS treatment as shown in Figure  
532 S11.



533

534 **Figure S11:**  $^1\text{H}$  NMR spectrum (300 MHz, 23 °C,  $\text{D}_2\text{O}$ ) of Fluor-Alg-Ph.

535

536

537

538

539

540

541

542

543

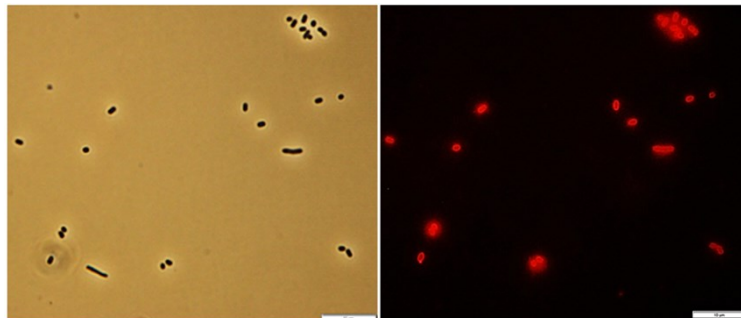
544

545

546

547 **Supplementary Figure 12: Immobilization of HRP-mCherry<sup>His</sup> on *E. coli* surface**  
548 **mediated by Fe<sup>3+</sup>**

549 The immobilization of HRP-mCherry<sup>His</sup> on the cell surface was inspected by fluorescence  
550 microscope. As shown in Figure S12, the cells were decorated with red fluorescence upon  
551 treatment with Fe<sup>3+</sup> and HRP-mCherry<sup>His</sup>, which indicates that HRP-mCherry<sup>His</sup> was  
552 successfully immobilized on the cell surface.

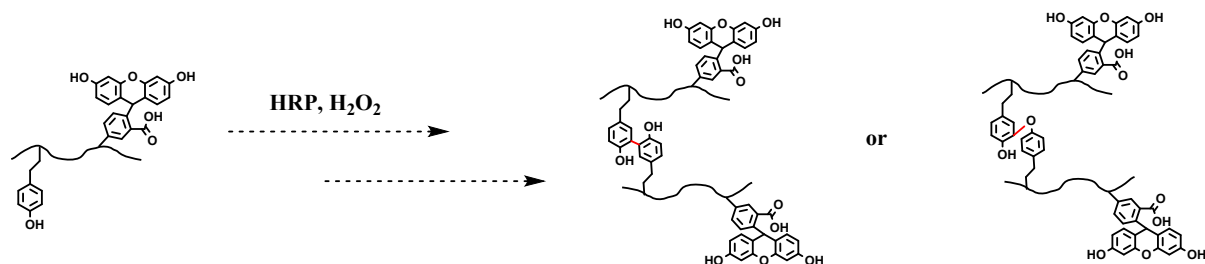


553  
554 **Figure S12:** Fluorescence images of HRP-mCherry<sup>His</sup> immobilized on the cell surface. The red fluorescence signal  
555 (mCherry) indicated the HRP-mCherry<sup>His</sup> was successfully immobilized on *E. coli* cell surface mediated by Fe<sup>3+</sup>.  
556 The image was inspected by fluorescence microscope in bright and red fields ( $\lambda_{\text{ex}} = 555 \text{ nm}$ ;  $\lambda_{\text{em}} = 640 \text{ nm}$ ) at the  
557 exposure time of 109.7 ms and the gain of 2.9 dB.

558  
559  
560  
561  
562  
563  
564  
565  
566  
567  
568  
569  
570  
571

572 **Supplementary Figure 13: Reaction scheme for hydrogel polymerization**  
573 **reaction initiated by HRP**

574 The biocompatible hydrogel polymerization was initiated by a peroxidase-catalyzed oxidation  
575 reaction <sup>11</sup>. The Fluor-Alg-Ph hydrogel was formed through the controlled radical  
576 polymerization using H<sub>2</sub>O<sub>2</sub> as an oxidant of horseradish peroxidase (HRP) to generate hydroxyl  
577 radical to initial the coupling of the phenol moiety.



578

579 **Figure S13:** Illustration for Fluor-Alg-Ph hydrogel formation initiated through H<sub>2</sub>O<sub>2</sub> and HRP.

580

581

582

583

584

585

586

587

588

589

590

591

592

593

594

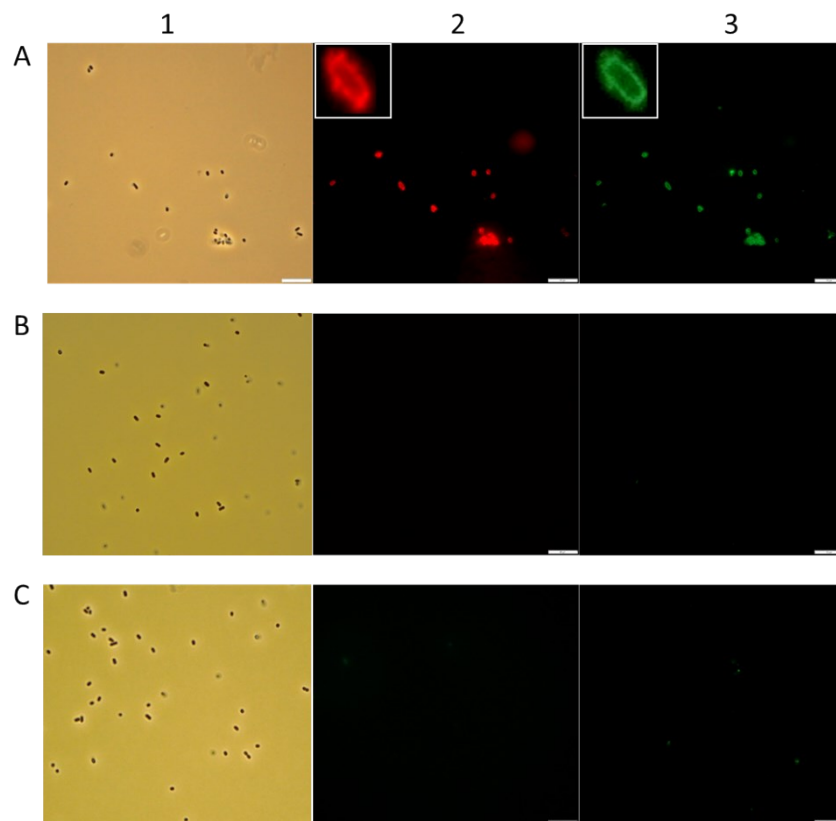
595

596



597 **Supplementary Figure 14: Fluorescence image of *E. coli* cells encapsulated in a**  
598 **conformal alginate shell**

599 *E. coli* cell encapsulation with alginate shell was inspected by fluorescence microscope. As  
600 shown in Figure S14, after soaking in the solution containing Fluor-Alg-Ph and H<sub>2</sub>O<sub>2</sub>, the  
601 hydrogel sheath was formed on the cells immobilized with HRP-mCherry<sup>His</sup> (Fig S14A). In  
602 contrast, the cells without Fe<sup>3+</sup> (treated with free HRP-mCherry<sup>His</sup> or commercial HRP (no His<sub>6</sub>-  
603 Tag) as shown in Fig S14 B and C) cannot form any hydrogel sheath around the cell surface.  
604 These results confirmed hydrogel formation occurred only on the cell surface carrying HRP-  
605 mCherry<sup>His</sup>.



606

607 **Figure S14:** Single cell encapsulation in conformal Fluor-Alg-Ph hydrogel sheath based on controlled radical  
608 polymerization using HRP-mCherry<sup>His</sup>. (A) Cells treated with HRP-mCherry<sup>His</sup> and Fe<sup>3+</sup> for hydrogel sheath  
609 formation. The red fluorescence from mCherry indicates HRP-mCherry<sup>His</sup> was still immobilized on *E. coli* cell  
610 surface after gel formation process ( $\lambda_{\text{ex}} = 555 \text{ nm}$ ,  $\lambda_{\text{em}} = 640 \text{ nm}$ ). The green fluorescence from 5-aminofluorescein  
611 indicates Fluor-Alg-Ph polymers are surrounded on *E. coli* cell surface ( $\lambda_{\text{ex}} = 470 \text{ nm}$ ,  $\lambda_{\text{em}} = 535 \text{ nm}$ ). Cells treated  
612 with HRP-mCherry<sup>His</sup> alone (B) or with commercial HRP alone (C) showed no hydrogel sheath around the cell  
613 surface. The pictures were inspected by fluorescence microscope in bright field (1), red field (2), and green field  
614 (3) at the exposure time of 109.7 ms and the gain of 2.9 dB.

615

616

617 **Appendix**

618 **Gene of** HRP-GGS-mCherry-His tag

619 CAGTTGACTCCAACCTTCTACGACAACCTCCTGTCCAAACGTTTCCAACATCGTCAGAGACACCATCGT  
620 CAACGAGTTGAGATCTGACCCAAGAATCGCTGCCTCCATCTTGAGATTGCACTTCCACGACTGTTTCG  
621 TGAACGGTTGTGACGCTTCCATCTTGTTGGACAACACCACTTCCTTCAGAAGGACGCTTTC  
622 GGTAACGCTAACTCTGCTAGAGGTTTCCCAGTCATCGACAGAATGAAGGCTGCTGTTGAATCCGCTTG  
623 TCCAAGAAGTGTTCCTGTGCTGACTTGTTGACTATCGCTGCTCAACAGTCCGTTACTTTGGCTGGTG  
624 GTCCATCTTGGAGAGTTCCATTGGGTAGAAGAGATTCTTGCAGGCCTTCTTGGATTTGGCTAACGCT  
625 AATTTGCCAGCTCCATTCTTACCTTGCCTCAGTTGAAGGACTCTTTCAGAAACGTCGGTCTGAACAG  
626 ATCCTCCGACTTGGTTGCTTTGTCTGGTGGACACACCTTTGGTAAGAACCAGTGCAGATTCATCATGG  
627 ACAGACTGTACAACCTTCTCCAACACCGGTTTGGCAGATCCAACCTTGAACACCACCTACTTGCAGACC  
628 TTGAGAGGTTTGTGTCCACTGAACGGTAACTTGTCCGCTTTGGTTGACTTCGACTTGAGAACCCCAAC  
629 TATCTTCGACAACAAGTACTACGTCAACTTGGAGGAACAGAAGGTTTGGATCCAATCCGACCAAGAGT  
630 TGTTCTCTTCCCAAACGCTACTGACACTATCCCATTGGTTAGATCCTTCGCCAACTCTACCCAGACT  
631 TTCTTCAACGCTTTCGTTGAGGCTATGGACAGAATGGGTAACATCACTCCATTGACCGGTACTCAGGG  
632 TCAGATTAGATTGAACTGCAGAGTCGTTAACGGAGCGGTGGTCCATGGTGAGCAAAGGTGAAGAGG  
633 ATAATATGGCCATCATCAAAGAATTTATGCGCTTTAAAGTGCACATGGAAGGTAGCGTTAATGGCCAT  
634 GAATTTGAAATTGAAGGTGAAGGCGAAGGTTCGTCCTATGAAGGCACCAGACCGCAAACTGAAAGT  
635 TACCAAAGGTGGTCCGCTGCCGTTTGCATGGGATATTCTGAGTCCGCAGTTTATGTATGGTAGCAAAG  
636 CCTATGTTAAACATCCGGCAGATATCCCGGATTATCTGAAACTGAGCTTTCGGGAAGGTTTTAAATGG  
637 GAACGTGTGATGAATTTTGAAGATGGTGGTGTGTTACCGTTACCCAGGATAGCAGCCTGCAGGATGG  
638 TGAATTTATCTATAAAGTTAAACTGCGTGGCACCATTTCGAGTGATGGTCCGGTTATGCAGAAAA  
639 AAACCATGGGTTGGGAAGCAAGCAGCGAACGTATGTATCCGGAAGATGGCGCACTGAAAGGTGAAATT  
640 AAACAGCGCCTGAAACTGAAAGATGGTGGCCATTATGATGCAGAAGTTAAAACCACCTATAAAGCCAA  
641 AAAACCGGTTTCCAGCTGCCTGGTGCATATAACGTTAACATTAACCTGGATATCACCAGCCACAACGAGG  
642 ATTATACCATTGTTGAACAGTATGAACGTGCAGAAGGTCGCCATAGTACCGGTGGTATGGATGAACTG  
643 TATAAACATCATCATCATCATCAC

644

645

646

647

648

649

650

651

652

653

654

655

656

## 657 References

- 658 1. N. Cruz, S. L. Borgne, G. Hernandez-Chavez, G. Gosset, F. Valle and F. Bolivar, *Biotechnol. Lett.*,  
659 2000, **22**, 7.
- 660 2. P. Komadel, *Clays and Clay Minerals*, 1988, **36**, 379-381.
- 661 3. K. Koschorreck, S. M. Richter, A. B. Ene, E. Roduner, R. D. Schmid and V. B. Urlacher, *Appl.*  
662 *Microbiol. Biotechnol.*, 2008, **79**, 217-224.
- 663 4. H. Y. Cui, T. H. J. Stadtmuller, Q. J. Jiang, K. E. Jaeger, U. Schwaneberg and M. D. Davari,  
664 *Chemcatchem*, 2020, **12**, 4073-4083.
- 665 5. S. Q. Meng, J. Guo, K. L. Nie, U. Schwaneberg, T. W. Tan, H. J. Xu and L. Liu, *J Biobased Mater Bio*,  
666 2019, **13**, 79-85.
- 667 6. B. Morawski, Z. L. Lin, P. C. Cirino, H. Joo, G. Bandara and F. H. Arnold, *Protein Eng*, 2000, **13**,  
668 377-384.
- 669 7. S. Sakai and K. Kawakami, *Acta Biomater*, 2007, **3**, 495-501.
- 670 8. Y. Liu, S. Sakai, S. Kawa and M. Taya, *Anal Chem*, 2014, **86**, 11592-11598.
- 671 9. J. Watly, E. Simonovsky, R. Wieczorek, N. Barbosa, Y. Miller and H. Kozlowski, *Inorg. Chem.*,  
672 2014, **53**, 6675-6683.
- 673 10. G. R. Fulmer, A. J. M. Miller, N. H. Sherden, H. E. Gottlieb, A. Nudelman, B. M. Stoltz, J. E.  
674 Bercaw and K. I. Goldberg, *Organometallics*, 2010, **29**, 2176-2179.
- 675 11. M. Kurisawa, J. E. Chung, Y. Y. Yang, S. J. Gao and H. Uyama, *Chem Commun* 2005, DOI:  
676 10.1039/b506989k, 4312-4314.

677